European Scholar Journal (ESJ)
Available Online at: https://www.scholarzest.com
Vol. 3 No.2, February 2022
ISSN: 2660-5562

ESTIMATION OF ARGON PLASMA PARAMETERS IN PB-ZN CO-SPUTTERING SYSTEM AT VARIOUS GAS PRESSURE

Aws Faisal Rauuf, Kadhim A. Aadim
Department of Physics, College of Science, University of Baghdad, Baghdad, Iraq
E-mail: aws.raouf1104@sc.uobaghdad.edu.iq

Article history:

Received: 7th December 2021
Accepted: 10th January 2022
Published: 18th February 2022

Abstract:

In this work, a planar DC sputter system was successfully designed, built, and assembled. Depending on the optical emission spectroscopy, the fundamental plasma parameters like electron temperature (T_e) and electrons density (n_e) have been measured using the Boltzmann plot method and Stark broadening with different gas pressures and distances 4 cm between the electrodes. Also, other plasma parameters: plasma frequency (ω_p), Debye length (λ_D), and the number of particles in the debye sphere (N_D), which are related to T_e and n_e were measured. It is found that the T_e, λ_D, and N_d decreases and n_e and ω_p increase with increasing the argon gas pressure.

Keywords: *Zinc-Lead plasma. Argon plasma. Sputtering. Co- sputtering. plasma parameters*

1. INTRODUCTION

For metal oxide and metal nitride surface coatings, co-sputtering is a common technique. It is superior in composition reproducibility and thinness on a large area substrate [1-3]. Due to the electric field, the cathode (material used for sputtering), pressure, the density of discharge power, and use sputter gas, the plasma discharge species are regulated in a particular ratio by the gas and metal reactions [4]. In the presence of a reactive gas, co-sputtering is called reactive co-sputtering. Typically, two different materials were sputtered using an Ion-beam or RF or DC equipment to power the sputtering of targets and create thin films. Sputter deposition is one of the most fundamental ways of preparation since alloy film composition can be adjusted and adherence to the substrate increased [5].

When plasma particles collide with electrons, they will be excited to higher electronic states. The cause of the emitted light photons is the relaxation of excited particles in the chamber at lower energy levels. The difference between excited and lower energy states corresponds to the energy of the emitted photon and is the wavelength of a spectral line indicated in the relationship:

$$\lambda = hc/\ E_j - E_i \qquad (1)$$

Where h is the Planck constant, c: speed of light, and E_j, E_i is the higher and the lower energy state, respectively. Since the energy of a transition is a defining feature of the particles, photon energy analysis can reveal the composition of the plasma.

This work aims to a spectroscopic diagnostic for Zn-Pb produced by co-sputtering technique.

2. EXPERIMENTAL PROCEDURE.

The experimental schematic setup of the Direct Current Co-sputtering system is shown in Fig. 1. The system is composed of a vacuum bell-jar chamber with an inner diameter of 29 cm and an inner height of 60 cm with 0.5cm thickness; the vessel includes two targets set as cathodes and one anode. The first target is made of Zinc metal and the other of lead metal with diameters 5 cm to each of them. Both targets are oriented 60° with a distance of 4 cm away from the anode. It is electrically connected to two DC power supplies. Argon gas purity content (99.999 %) was used as plasma gas, with vacuum pressure ranged (0.1, 0.2, 0.3, 0.4) mbar. The discharge voltage has been applied to the targets at 1000 Volts. The argon discharge between the electrodes was created when the DC voltage was applied. Spectra emission of the discharge was collected by optical fibre connected with a spectrometer. The optical emission lines of Ar spectrum results were measured using the NIST [6] database software to estimate the Ar plasma characteristics.

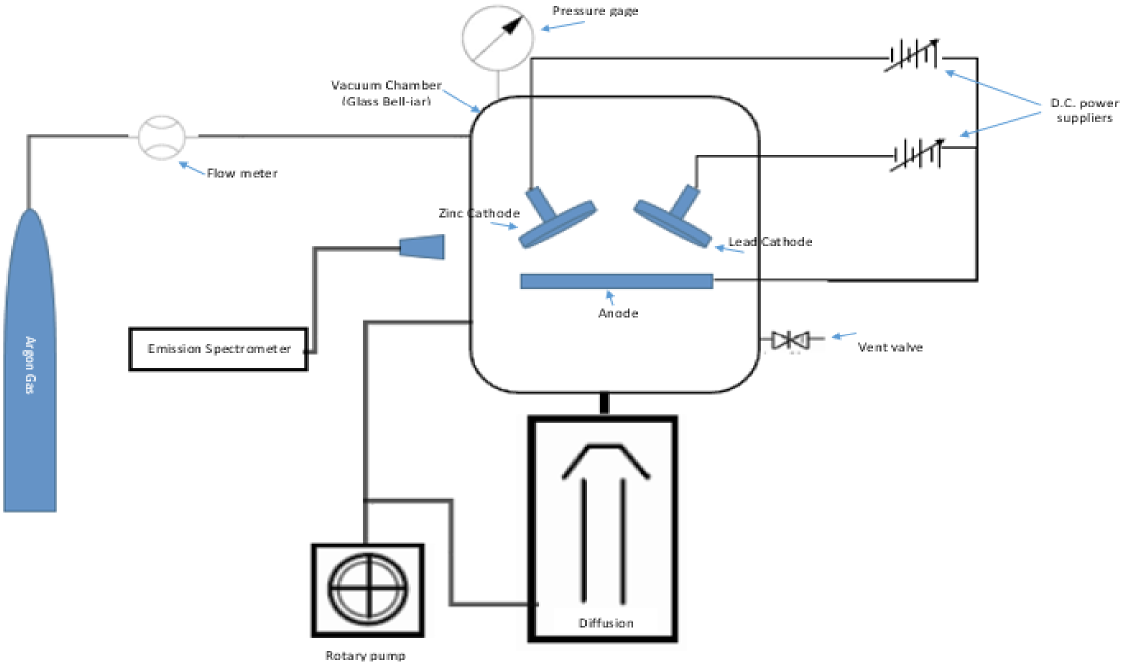

Fig.1: schematic diagram of DC Co-sputtering system.

Table 1. Values of the Transitions probability, statistical weight and upper energy level of a spectral line emitted from Ar plasma [6].

Emission lines	λ (nm)	g_kA_{ik} (s^{-1})	$E_k(eV)$
Ar I	696.5	1.9×10^7	13.32
	763.5	1.22×10^8	13.17
	801.4	4.6×10^7	13.09
	811.5	2.3×10^8	13.07

3. RESULTS AND DISCUSSION

Plasma spectroscopy, focusing on low-temperature plasma-atomic and molecular emission spectroscopy, is a powerful diagnostic tool for Ar plasmas parameter determination, especially in the UV/visible region for neutral gas temperature determination. The light intensity measurement gives a qualitative indication of the concentration of species involved in optical emissions. Collisions of excitation and decay in radiative species emit plasma species characteristics that can be detected and analyzed as optical emission spectroscopy (OES) [7]. The plasma emission intensities provide information about the plasma species concentration. The data provided in Table 1 have been used in this study and discussion of spectral lines emitted atoms. Depending on the optical emission spectra (OES) of the Ar sputtering plasmas, the behaviour of the Argon plasma in a vacuum has been investigated, as shown in Fig.2.

Characteristic OES spectra of plasma taken in the wavelength region of 250 – 950 nm are displayed in Fig. 2. The emission lines appearing in the spectra are assigned according to neutral ZnI, PbI ArI, and ions ZnII, PbII, ArII emission lines dominate the OES spectra.

Fig. 2. shows the emission spectra of Zn-Pb plasma recorded in the wavelength range from 250 to 950 nm as a function of gas pressure (0.2-0.5 mbar). It is found that the plasma intensity decreases with pressure decrease.

Figure 2. The intensity of optical emission spectroscopy of Zinc-Lead DC Co-sputtering plasma for various Argon pressure.

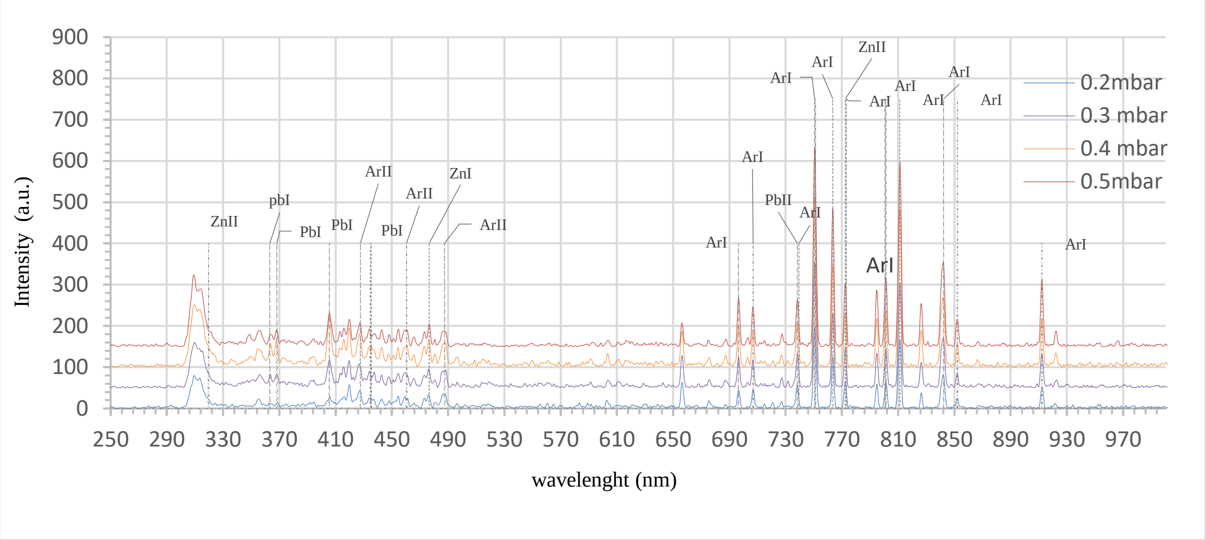

In sputtering, as electrons get accelerated and gain energy from the power source, they transfer part of this energy to atoms, ions, and molecules, if present in the plasma through collisions. Hence, information about electron energy distribution is essential to control chemical or physical processes in plasma better. The concept of electron temperature is applicable if electrons are in thermal equilibrium with each other. The density of argon species is lower at low pressure, and the mean free path of free electrons is longer, and this pathway is not large enough to accelerate free electrons as pressure is increased. As a result, emission intensities increase and collisions between plasma species and electrons increase, raising the temperature of the species while lowering the temperature of the electrons. Hence, electron energy distribution's high tail is quenched; these results agree with [8].

The lines of Argon spectra listed in table 1 are used to obtain the plasma parameters (T_e, n_e, ω_p, λ_D, and N_D). The Boltzmann plot method can be used to measure the temperature of the electron. As shown in the equation below, the atomic emission intensity (Iji) of the transition from level j to level i is governed by the transition probability (Aji) and the absolute populations of the atomic level (Nj) [9]:

$$\ln\left(\frac{I_{Ji}\,\lambda_{ji}}{A_{ji}g_i}\right) = -\frac{E_j}{K_\beta\, T_e} + cons. \qquad (2)$$

Then

$$K_\beta\, T_e = -\frac{E_j}{\ln\left(\frac{I_{Ji}\,\lambda_{ji}}{A_{ji}g_i}\right)} \qquad (3)$$

Where λ_{ji} is the wavelength of the corresponding transition, g_j is the statistical weight of level j, Ej is its energy in cm^{-1}, k_B is the Boltzmann constant, and T_e is the electron temperature in Kelvin.

The electron density (ne) was determined by Saha equation, based on the electron temperature calculated from Fig. 5. The Saha equation is shown in formula (4): [10]:

$$n_e = 2\left(\frac{m_e kT}{2\pi h^2}\right)^{\frac{3}{2}} \frac{I_a\lambda_a}{I_i\lambda_i}\frac{A_i g_i}{A_a g_a}\; e^{-(E_{ion}+E_i-E_a)/T_e} \qquad (4)$$

Where me is electron mass, h is the Planck constant; subscript a, i represents atom and univalent ion respectively; Eion is the ionization energy. Argon atom and ion lines (Ar I: 751.46nm and Ar II: 810.36 nm) were used to calculate the electron density.

Debye's length (λ_D) can be calculated from the formula(5) [11]:

$$\lambda_D = \left(\frac{\varepsilon_o\, KT_e}{n_e\, e^2}\right)^{1/2} \qquad (5)$$

Electron's density and temperatures as a function of gas pressure are presented in Fig. 3. The results show that the electron temperatures decrease with the increased gas pressure, while the electron density increases with gas pressure. These results illustrate the evaluation of electron temperature and density as a function of supplied power and pressure. According to the observations, as supplied power rises, electron temperature and density rise due to inelastic collisions of electrons achieving sufficient energy to cause argon atom excitation and ionization. The energy of secondary electrons increases the excitation cross-section and decreases as electron energy increases.

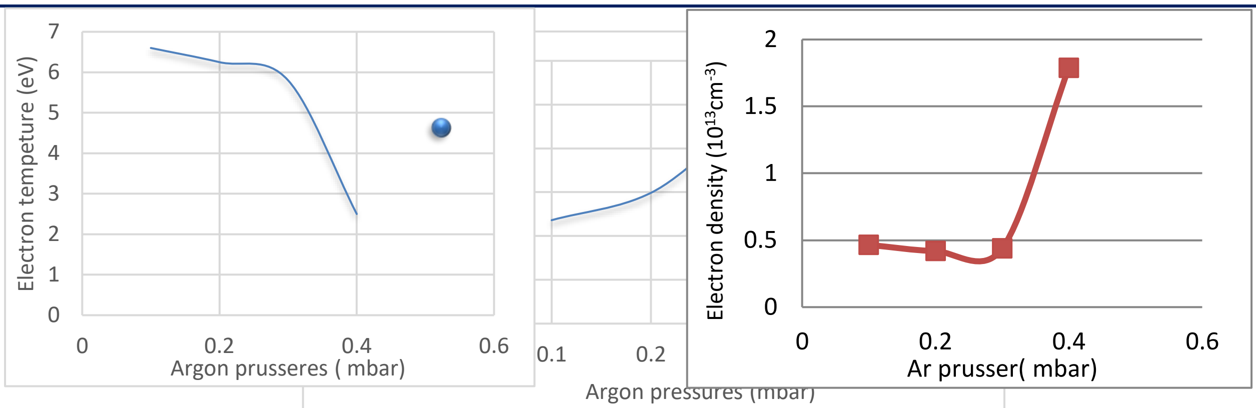

Fig.3: Electron temperatures and electron densities as a function of Argon pressure.

The number of particles in the Debye sphere N_D must be significant so that collecting interactions dominate at the average distance from the interparticle. The number of particles (N_D) in the air as well as under vacuum is calculated by the formula(6) [11]:

$$N_D = \frac{4\pi}{3} N_E \lambda_D^3 \qquad (6)$$

Debye length λ_D is the measure of the penetration depth of the external electrostatic domains, i.e. the boundary sheath thickness over which the neutrality of the charge cannot be maintained. Therefore, the applied electrical potential will develop mostly near surfaces over a distance of λ_D, which is a function of the electron and ion temperature and plasma density.

Debye length was evaluated by substituting the experimental data of T_e and ne into the equation (5). The number of particles (N_D) in a Debye sphere was calculated using equation 6.

Debye length increases with the increase of the electron temperature and decreases with increased gas pressure as well as N_D decreases with increased gas pressure, as shown in Figs .4.

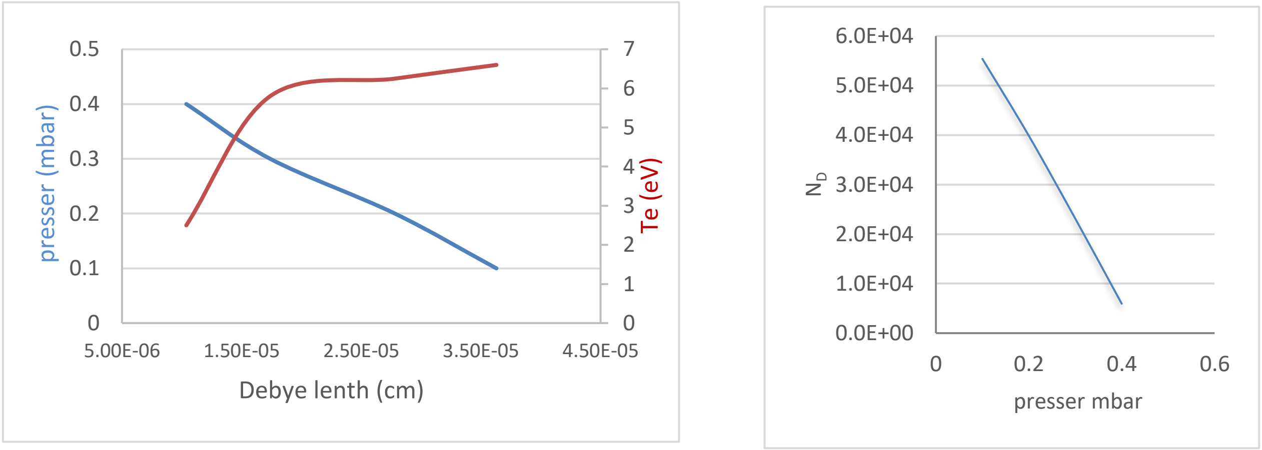

Fig.4. Debye lengths and number of particles as a function of pressure

The relatively fast electron frequency ω_{pe} (the ions do not participate in these oscillations because of their high mass) is the most important reference to the plasma frequency. Plasma oscillations will only be observed if the plasma system is studied over the periods τ longer than the $\tau = 1/\omega_{pe}$ and if external actions change the system at a rate no faster than ω_{pe}. Plasma frequency (ω_{pe}) can be calculated as [12].

$$\omega_{pe} = \sqrt[2]{\frac{e^2 n_e}{\varepsilon_o m_e}} \qquad (7)$$

The study of electron plasma frequency ω_p is significant. Any electric field applied below the plasma frequency has no penetrating the plasma body, as the electrons move fast enough to shield it out immediately. The medium's behaviour will be determined primarily by collective plasma phenomena, the fundamental plasma length, and time scales. Fig.5 shows the plasma frequency increase with the increase of gas pressure.

Fig.5. Plasma frequency as a function of pressure.

4. CONCLUSION.

In this work, the OES diagnostic was installed and tested to investigate the plasma parameters in the cylindrical DC co-sputtering apparatus. Using this technique at the low temperature, a weakly argon plasma was recorded. The results we get are the electron temperatures and electron densities increase with the pressure increase. The increase of spectral lines intensity correlates with the increase of the concentration of particles emitting the light from the plasma volume and the pressure increase. Finally, the electron densities have an increase with increasing the pressure, that reasons are illustrated above.

ACKNOWLEDGEMENTS.

The authors would like to thank the University of Baghdad, College of Science,
Department of Physics, Plasma laboratory staff for technical assistance during the research work.

CONFLICT OF INTEREST.

The authors declare that they have no conflict of interest.

REFERENCES

1. David A. Glocker and S. Ismat Shah, Handbook of Thin Film Process Technology. 2017: CRC Press, Taylor and Francis group.
2. M. Suhail, K. Adim and A. Wanas., On the Plasma Parameters in Co-sputtering Discharge. Br. J. Appl. Sci. Technol., 2015. 7, 3: pp. 263-279.
3. Nikolay Britun. And Jaroslav Hnilica. , Optical spectroscopy for sputtering process characterization. J. Appl. Phys, 2020. 127: pp. 211101
4. A. K. Singh, N. Kumari and P. K. Barhai., Study of RF/DC Co-Sputtered TiAlN Plasma Using Langmuir Probe for Prospective Industrial Applications. International Journal of Engineering Research & Technology (IJERT),2013. 2, 12: pp 2284–2293.
5. Rabah Abdul Hamid Edan, Spectroscopic Study for Plasma Parameters Generated by D.C. Co-sputtering System. thesis 2017, university of Baghdad.
6. Mohammed Oudah Salman, Simulation and Experimental Study for the effects of operating conditions on the Interactions Within Direct Current Discharge Plasma, thesis 2017, University of Baghdad.
7. Kadhim A. Aadim, Simulation and experimental study of Pin-Plate DC discharge plasma technique. Iraqi Journal of Physics, 2017 Vol.15, No.34: PP. 138147
8. H. Shakeel, M. Mumtaz, S. Shahzada, a Nadeem, and S. U. Haq, spectroscopic characterization of laser ablated silicon plasma, Plasma Sources Sci. Technol.,2014. 23, 3: PP. 035006.
9. A. P. Rao, M. Gragston, a. K. Patnaik, p. S. Hsu and m. B. Shattan, Measurement of electron density and temperature from laser-induced nitrogen plasma at elevated pressure (1–6 bar). Optics Express,2019. Vol.27, No.23: PP. 33780- 33788
10. Y. Zhan, X. Yi, Z. Zhang, Z. Liu, Y. Geng, J. Wang, W. Wang, G. Li, X. Wang., Electron temperature and electron density of copper vacuum arc in diffuse arc mode and anode spot arc mode,in 2016 27th International Symposium on Discharges and Electrical Insulation in Vacuum (ISDEIV), 2016. IEEE.
11. Kadhim A. Aadim and Rabah A. H. Edan, spectroscopic study for plasma parameters in co-sputtering system. Iraqi Journal of physics vol.14 no.31 (2016) 122–128
12. A. F. Rauuf., Construction and Study of Atmospheric Plasma Jet Induced by Microwave. Thesis 2016. Baghdad University.